Eur. Phys. J. C (2022) 82:295
https://doi.org/10.1140/epjc/s10052-022-10210-6

THE EUROPEAN PHYSICAL JOURNAL C

Regular Article - Theoretical Physics

The $\mu \to e\gamma$ decay in an EW-scale non-sterile RH neutrino model

D. N. Dinh[a]

Institute of Physics, Vietnam Academy of Science and Technology, 10 Dao Tan, Hanoi, Vietnam

Received: 19 December 2021 / Accepted: 12 March 2022

Abstract We investigate herein the phenomenology of $\mu \to e\gamma$ decay in a scenario of the class of extended models with non-sterile right-handed (RH) neutrinos at electroweak (EW) scale proposed by P. Q. Hung. The field content of the standard model (SM) is increased by introducing for each SM fermion a corresponding mirror partner with the same quantum numbers along with opposite chirality. Light neutrino masses are generated via the type I seesaw mechanism, and it is also proved to be relevant to low energy within the EW scale of RH neutrino masses. We introduce the model and derive the branching ratio of the $\mu \to e\gamma$ decay at one-loop approximation with the participation of W gauge boson and neutral and singly charged Higgs scalars. We then set constraints on relevant parameters and predict the sensitivity of the decay channel under the present and future experiments.

1 Introduction

The electroweak-scale right-handed neutrino (EW-scale ν_R) model is an extended version of the standard model (SM) that was proposed for the first time in [1]. The fermion content is doubled by introducing a mirror partner for each of the SM particles, thus corresponding to a mirror component of the normal fermion, with opposite chirality. To obey the mirror symmetry, right-handed mirror neutrinos and leptons, for example, are combined to form a doublet of the model's gauge symmetry $SU(2) \times U(1)_Y$. Other particles in the mirror sector are arranged in a similar way.

With left-handed and right-handed neutrinos introduced in the normal and mirror sectors, respectively, adequate conditions are acquired for the type I seesaw mechanism operating to give masses for light active neutrinos [2–5]. In contrast to the normal type I seesaw, in which the Dirac mass matrix is generated at electroweak scale, and therefore right-handed neutrino masses should generally be extremely heavy to ensure SM active neutrino masses as small as experiments have identified, the Dirac mass matrix in the current model is given by a new Higgs singlet apart from the mechanism of SM mass production. It is proved that if the vacuum expectation value (VEV) of the Higgs singlet is at relevant scale, the heavy Majorana mass matrix is about 100 GeV, and thus at the EW scale [1].

Apparently, the mirror partners of the SM matter particles introduced in this model, which may affect various physical phenomena, have to confront the experimental high-precision measurements of the EW processes. The effects of extra chiral doublets were carefully examined in [6]. The research shows that there is still large free parameter space after being constrained by the EW precision data. One of the exciting explanations that has been demonstrated is the partial cancellation of the contributions from the mirror fermions by those of the physical scalars, especially the $SU(2)$ triplets. An updated version was introduced after the discovery of the 125 GeV SM-like scalar [7,8], which has opened a new stage for elementary particle physics, particularly model building for physics beyond the SM. Unlike the old version, an additional Higgs doublet has been introduced to give masses for mirror quarks and charged leptons (mirror sector), and the original one for those of the normal sector. Two candidates are found to have signals in agreement with ATLAS and CMS observations [9].

Despite compelling evidence for lepton flavor violations (LFV) in neutrino oscillations, all efforts searching for those in the charged lepton sector have given negative results so far. In fact, it has been demonstrated that with minimal extensions of the SM with massive neutrinos, the rates of LFV processes involving the charged leptons are so tiny that they are unobservable in practice. For instance, the $\mu \to e\gamma$ decay branching ratio is estimated at about 10^{-55} using the currently known neutrino oscillation data [10–12]. For this reason, the decay is considered one of the most important channels in looking for signals of physics beyond the SM. From the experimental perspective, the best upper limit is implied

[a] e-mail: dndinh@iop.vast.vn (corresponding author)

Published online: 04 April 2022

from the non-observation of the muon decay $\mu \to e\gamma$ given by MEG in 2016 [13]

$$\mathrm{BR}(\mu^+ \to e^+\gamma) < 4.2 \times 10^{-13}, \tag{1}$$

and it was recently upgraded to work at sensitivity [14,15]

$$\mathrm{BR}(\mu^+ \to e^+\gamma) < 6.0 \times 10^{-14}. \tag{2}$$

From the theoretical perspective, a large number of studies have investigated the same topic in various scenarios of physics beyond the SM [10–12,16–30]. Among them, the $\mu \to e\gamma$ branching ratios and related consequences in the schemes of EW-scale ν_R models considered are discussed for three different versions, namely the original [25], the updated with light of the 125 GeV SM-like Higgs scalar discovery [26], and an extension with A_4 discrete symmetry [27].

Although the phenomenology of $\mu \to e\gamma$ decay in the three abovementioned EW-scale ν_R scenarios has been considered, these studies have only taken into account the contributions of one-loop diagrams, which are formed by the light neutral scalar and the mirror charged leptons. The theoretically predicted branching ratio confronted with the experimental upper bound will set upper limits on the magnitudes of Yukawa couplings involving the Higgs singlet. Following that, the light singlet vacuum expectation value v_s is identified to have right Dirac mass magnitude for the seesaw mechanism working properly with 100 GeV Majorana right-handed neutrino masses to generate sub-eV scale of those for the light active neutrinos. However, this is only part of the whole story. At one-loop approximation, there are still contributions from diagrams with W^- gauge bosons and other neutral and singly charged scalars. These contributions may be sizable, and therefore careful consideration must be given to set constraints on the interaction strengths involved or to evaluate their observed possibilities with the current and future experiments.

As the aim of this study, we discuss the phenomenology of $\mu \to e\gamma$ decay in the scenario of the EW-scale ν_R model with two Higgs doublets, with the extended version to accommodate the 125 GeV SM-like scalar detection [9,26]. The process is considered up to one-loop approximation with participation of light physical scalar and other particles, which have not been studied in the previous works. The paper is divided into four main sections as follows. After the introduction presented in this section, in Sect. 2 we briefly introduce the model and present the relevant LFV vertexes which contribute to our process of interest. In Sect. 3, after introducing the form factors with explicit algebraic expressions, we derive the decay branching ratio and perform numerical analysis. The conclusion is given in Sect. 4.

2 A review of the model

2.1 The model content

As mentioned above, this study investigates an extended version of the EW-scale ν_R model, which is constructed based on the symmetric group $SU(2) \times U(1)_Y \times U(1)_{SM} \times U(1)_{MF}$. The $SU(2) \times U(1)_Y$ is the gauge group of the model, and $U(1)_{SM} \times U(1)_{MF}$ is a global symmetry introduced to forbid some unexpected interactions. Matter fields are arranged as follows under the gauge group:

SM particles	Mirror particles
$\ell_L = (\nu_L,\ e_L)^{\mathrm{T}},\ e_R$	$\ell_R^M = (\nu_R,\ e_R^M)^{\mathrm{T}},\ e_L^M$
$q_L = (u_L, d_L)^{\mathrm{T}},\ u_R, d_R$	$q_R^M = (u_R^M,\ d_R^M)^{\mathrm{T}},\ u_L^M, d_L^M.$

With this choice, in contrast to the SM, right-handed neutrinos are components of $SU(2) \times U(1)_Y$ doublets; therefore, they are non-sterile and take part in the weak interaction.

Two SM-like Higgs doublets are introduced to give masses to the charged and mirror fermions, respectively. One Higgs doublet, which is denoted as $\Phi_2 = (\phi_2^+, \phi_2^0)$, couples to the SM fermions to produce their masses, while the other, denoted as $\Phi_{2M} = (\phi_{2M}^+, \phi_{2M}^0)$, is responsible for the mass generation of the matter partner particles in the mirror sector. The mechanisms of lepton mass generation, including both charged leptons and neutrinos, will be presented in detail later in the paper.

The heavy right-handed neutrinos in this model are introduced naturally in the mirror sector; therefore, light active neutrino masses are generally expected to be generated by the type I seesaw mechanism. The right-hand neutrino mass matrix is provided by a complex Higgs triplet with $Y = 2$

$$\tilde{\chi} = \frac{1}{\sqrt{2}}\boldsymbol{\tau}.\boldsymbol{\chi} = \begin{pmatrix} \frac{1}{\sqrt{2}}\chi^+ & \chi^{++} \\ \chi^0 & -\frac{1}{\sqrt{2}}\chi^+ \end{pmatrix}. \tag{3}$$

If only one triplet, e.g. $\tilde{\chi}$, is introduced in the model, the tree-level result $\rho = 1$, which is precisely measured by experiment, will be spoiled, and then one might obtain $\rho = 2$ instead. However, it is also proven in [31] that if one has two triplets with relevant hyper-charges, when combined to form $(3, 3)$ representation under the global $SU(2)_L \otimes SU(2)_R$ symmetry, the custodial $SU(2)$ symmetry is preserved and $\rho = 1$. Thus, along with the triplet $\tilde{\chi}$, it is necessary to add a real Higgs triplet with $Y = 0$, denoted as (ξ^+, ξ^0, ξ^-). Finally, we introduce the SM singlet Higgs ϕ_S, which is responsible for creating the Dirac mass matrix and connection between the matter and mirror sectors.

In this model, two Higgs doublets Φ_2 and Φ_{2M} are used to couple to the SM and mirror fermions, respectively. To prevent unexpected couplings, global symmetries $U(1)_{SM} \times U(1)_{MF}$ are imposed. The transformations of matter and Higgs fields are defined as follows:

(i) $U(1)_{SM} : \Psi = \{\Phi_2,\ q_L^{SM},\ \ell_L^{SM}\}$ transforms as $\Psi \to e^{i\alpha_{SM}}\Psi$,
(ii) $U(1)_{MF} : \Psi = \{\Phi_{2M},\ q_R^{M},\ \ell_R^{M}\}$ transforms as $\Psi \to e^{i\alpha_{MF}}\Psi$,
(iii) $\phi_S \to e^{-i(\alpha_{MF}-\alpha_{SM})}\phi_S$, $\tilde{\chi} \to e^{-2i\alpha_{MF}}\tilde{\chi}$, and the unmentioned fields are singlet under this global symmetry.

Before presenting the Yukawa couplings, we should keep in mind that the global symmetry defined above only allows Φ_2 to couple to SM fermions, while Φ_{2M} will couple to the mirror ones. Apparently, terms involving ϕ_S should contain both SM and mirror fermion fields. Two unit lepton number violation terms, which are needed to acquire Majorna mass for the operation of the seesaw type I, can only be constructed with the present of $\tilde{\chi}$. The Yukawa couplings are expressed in detail as follows:

$$\mathcal{L}_Y^{\ell} = g_{\ell}\bar{\ell}_L\Phi_2 e_R + g_{\ell}^M\bar{\ell}_R^M\Phi_{2M}e_L^M + g_{\ell s}\bar{\ell}_L\phi_s\ell_R^M + \text{h.c.}, \tag{4}$$

$$\mathcal{L}_Y^{q} = g_u\bar{q}_L\tilde{\Phi}_2 u_R + g_d\bar{q}_L\Phi_2 d_R + g_u^M\bar{q}_R^M\tilde{\Phi}_{2M}u_L^M + g_d^M\bar{q}_R^M\Phi_{2M}d_L^M + g_{qs}\bar{q}_L\phi_S q_R^M + \text{h.c.}, \tag{5}$$

$$\mathcal{L}_{\nu_R} = g_M l_R^{M,T}\,\sigma_2\,\tilde{\chi}\,l_R^M, \tag{6}$$

where σ_2 is the second Pauli matrix, $\tilde{\Phi}_2 = i\sigma_2\Phi_2^*$ and $\tilde{\Phi}_{2M} = i\sigma_2\Phi_{2M}^*$.

2.2 Symmetry breaking and mass generation

We will next discuss the mechanism of mass generation for matter particles in this model, especially for leptons including both charged leptons and neutrinos which are involved in later discussions of the research, when the symmetry is spontaneously breaking. For further discussion, we suppose that Higgs fields develop their VEVs as follows: $\langle\Phi_2\rangle = (0, v_2/\sqrt{2})^{\mathrm{T}}$, $\langle\Phi_{2M}\rangle = (0, v_{2M}/\sqrt{2})^{\mathrm{T}}$, $\langle\chi^0\rangle = v_M$, and $\langle\phi_S\rangle = v_S$.

The charged lepton mass matrix obtained from Eq. (4) can be expressed as

$$M_{\ell} = \begin{pmatrix} m_{\ell} & m_{\ell}^D \\ (m_{\ell}^D)^{\dagger} & m_{\ell M} \end{pmatrix}, \tag{7}$$

where $m_{\nu}^D = m_{\ell}^D = g_{\ell s}v_S$, $m_{\ell} = g_{\ell}v_2/\sqrt{2}$, and $m_{\ell M} = g_{\ell}^M v_{2M}/\sqrt{2}$. The matrix shown in Eq. (7) can be diagonalized to give eigenvalues in the mass basis and mixing matrix for the charged lepton. Without the loss physical reality, and for easier calculation to obtain the algebraic expression of the mixing matrix, let us assume that $m_{\ell M} \gg m_{\ell}$ and $m_{\ell M}, m_{\ell} \gg m_{\ell}^D$. The assumption allows us to approximately block diagonalized M_{ℓ} in the same way usually done for the seesaw type I neutrino mass matrix. Then we have

$$M_{\ell} = \begin{pmatrix} I & R_{\ell} \\ -R_{\ell}^{\dagger} & I \end{pmatrix}\begin{pmatrix} \tilde{m}_{\ell} & 0 \\ 0 & \tilde{m}_{\ell M} \end{pmatrix}\begin{pmatrix} I & R_{\ell} \\ -R_{\ell}^{\dagger} & I \end{pmatrix}^{\dagger}, \tag{8}$$

where $R_{\ell} \approx \frac{m_{\ell}^D}{m_{\ell M}} \ll 1$, and

$$\tilde{m}_{\ell} = m_{\ell} - \frac{(m_{\ell}^D)^2}{m_{\ell M} - m_{\ell}} \approx m_{\ell}, \tag{9}$$

$$\tilde{m}_{\ell M} = m_{\ell M} + \frac{(m_{\ell M}^D)^2}{m_{\ell M} - m_{\ell}} \approx m_{\ell M}. \tag{10}$$

Suppose that normal and mirror charged lepton matrices are written in the form $\tilde{m}_{\ell} = U_{\ell L}m_{\ell}^d U_{\ell R}^{\dagger}$, $\tilde{m}_{\ell M} = U_{\ell L}^M m_{\ell M}^d U_{\ell R}^{M\,\dagger}$, where m_{ℓ}^d and $m_{\ell M}^d$ are diagonal. We have the relation between the gauge states and physical states as follows:

$$\begin{pmatrix} \ell_{L(R)} \\ \ell_{L(R)}^M \end{pmatrix} = \begin{pmatrix} U_{\ell L(R)} & -R_{\ell}U_{\ell L(R)}^M \\ R_{\ell}^{\dagger}U_{\ell L(R)} & U_{\ell L(R)}^M \end{pmatrix}\begin{pmatrix} \ell'_{L(R)} \\ \ell^{M'}{}_{L(R)} \end{pmatrix}. \tag{11}$$

Similarly, we have the quark mass matrix

$$M_q = \begin{pmatrix} m_q & m_q^D \\ (m_q^D)^{\dagger} & m_{qM} \end{pmatrix}, \tag{12}$$

noting that $m_q^D = g_{qs}v_S$, $m_q = g_q v_2/\sqrt{2}$, and $m_{qM} = g_q^M v_{2M}/\sqrt{2}$. Block diagonalization gives us

$$\tilde{m}_q = m_q - \frac{(m_q^D)^2}{m_{qM} - m_q}, \tag{13}$$

$$\tilde{m}_{qM} = m_{qM} + \frac{(m_{qM}^D)^2}{m_{qM} - m_q}. \tag{14}$$

The quark sector will not be further discussed, because they are not involved in the LFV decays being considered in this research.

Denoting the heavy Majorana mass matrix as $M_R = g_M v_M$, one easily obtains the full neutrino mass matrix, which has the canonical form of the type I seesaw mechanism

$$M_{\nu} = \begin{pmatrix} 0 & m_{\nu}^D \\ (m_{\nu}^D)^{\mathrm{T}} & M_R \end{pmatrix}. \tag{15}$$

With block diagonalization of the matrix, it can be rewritten as follows, for $M_R \gg m_{\nu}^D$,

$$M_{\nu} = \begin{pmatrix} I & R_{\nu} \\ -R_{\nu}^{\dagger} & I \end{pmatrix}\begin{pmatrix} \tilde{m}_{\nu} & 0 \\ 0 & \tilde{m}_{\nu R} \end{pmatrix}\begin{pmatrix} I & R_{\nu} \\ -R_{\nu}^{\dagger} & I \end{pmatrix}^{\mathrm{T}}, \tag{16}$$

where $R_{\nu} \approx \frac{m_{\nu}^D}{M_R}$, and

$$\tilde{m}_{\nu} \approx -\frac{(m_{\nu}^D)^2}{M_R} = -\frac{(g_{\ell s}v_S)^2}{g_M v_M}, \quad \tilde{m}_{\nu R} \approx M_R. \tag{17}$$

In contrast to Eq. (8), where the charged lepton mass matrix $M = M^{\dagger}$ is Hermitian, thus being transformed by a unitary matrix and its conjugated matrix, the complex symmetric

$M_\nu = M_\nu^{\mathrm{T}}$ is rotated by a unitary matrix and its orthogonal matrix (see Eq. (16)). The light neutrino mass matrix $\tilde{m}_\nu$ is experimentally constrained to be smaller than 1 eV; if $(g_{\ell s}^2/g_M) \sim O(1)$ and $v_S \sim O(10^5$ eV), the Majorana mass of the right-handed neutrino M_R could be at the order of the electroweak scale. The electroweak scale right-handed neutrino mass is the most interesting scenario that could be designed in the considered model; however, M_R is not forbidden to have value in other ranges, depending on both the magnitude of v_M and interaction strength g_M. Consequently, v_S will vary in a corresponding range to give a right-handed light active neutrino mass matrix. Moreover, $g_{\ell s}$ is constrained by some rare processes (for instance, $\mu \to e\gamma$ decay, as we will see later), which might lead to constraint $(g_{\ell s}^2/g_M) \ll 1$. In this case, v_S would need to be at the order of GeV or higher, if neutrino mass generation is chosen to operate at the electroweak scale. For this reason, in this study, v_S is considered in a large range from hundreds of keV to a few tens of GeV.

Suppose that light and heavy (mirror) neutrino mass matrices are written respectively as $\tilde{m}_\nu = U_\nu^* m_\nu^d U_\nu^\dagger$, $\tilde{m}_{\nu R} = U_\nu^{M*} m_{\nu M}^d U_\nu^{M\dagger}$, where m_ν^d and $m_{\nu M}^d$ are diagonal, we easily obtain

$$\begin{pmatrix} \nu_L \\ (\nu_R)^c \end{pmatrix} = \begin{pmatrix} U_\nu & -R_\nu U_\nu^M \\ R_\nu^\dagger U_\nu & U_\nu^M \end{pmatrix} \begin{pmatrix} \chi_\nu \\ \chi_M \end{pmatrix}. \tag{18}$$

To guarantee $\rho = 1$, as mentioned above, the Higgs potential should have a global symmetry $SU(2)_L \otimes SU(2)_R$, and it is broken down to the custodial $SU(2)$ when the Higgs fields gain their VEVs. Before the symmetry is broken, two triplets combine to form the (3, 3) representation and the doublets also maintain the (2, 2) structures under the global symmetry. The detailed expressions are as follows:

$$\chi = \begin{pmatrix} \chi^0 & \xi^+ & \chi^{++} \\ \chi^- & \xi^0 & \chi^+ \\ \chi^{--} & \xi^- & \chi^{0*} \end{pmatrix}, \tag{19}$$

$$\Phi_2 = \begin{pmatrix} \phi_2^{0,*} & \phi_2^+ \\ \phi_2^- & \phi_2^0 \end{pmatrix}, \quad \Phi_{2M} = \begin{pmatrix} \phi_{2M}^{0,*} & \phi_{2M}^+ \\ \phi_{2M}^- & \phi_{2M}^0 \end{pmatrix}. \tag{20}$$

From the above equations, one have the proper vacuum alignment for breaking gauge symmetry from $SU(2)_L \times U(1)_Y$ to $U(1)_{em}$

$$\langle \chi \rangle = \begin{pmatrix} v_M & 0 & 0 \\ 0 & v_M & 0 \\ 0 & 0 & v_M \end{pmatrix}, \tag{21}$$

$$\langle \Phi_2 \rangle = \begin{pmatrix} \frac{v_2}{\sqrt{2}} & 0 \\ 0 & \frac{v_2}{\sqrt{2}} \end{pmatrix}, \quad \langle \Phi_{2M} \rangle = \begin{pmatrix} \frac{v_{2M}}{\sqrt{2}} & 0 \\ 0 & \frac{v_{2M}}{\sqrt{2}} \end{pmatrix}. \tag{22}$$

Thus, the VEVs of real components of Φ_2, Φ_{2M} and χ are $(v_2/\sqrt{2})$, $(v_{2M}/\sqrt{2})$ and v_M, respectively, and they satisfy the condition

$$v_2^2 + v_{2M}^2 + 8\, v_M^2 = v^2, \tag{23}$$

where $v \approx 246$ GeV. For further discussion, the following definitions are used:

$$s_2 = \frac{v_2}{v}; \quad s_{2M} = \frac{v_{2M}}{v}; \quad s_M = \frac{2\sqrt{2}\, v_M}{v}. \tag{24}$$

After gauge symmetry is spontaneously broken, the left-right global symmetry of the Higgs potential is also broken down to the custodial $SU(2)_D$. Seventeen degrees of freedom of the two Higgs triplets (one real and one complex) and two Higgs doublets are rearranged into physical Higgs bosons, and three of the Nambu–Goldstone bosons are absorbed to give masses for W's and Z. Among the physical bosons, those which have degenerate masses are grouped in the same physical scalar multiplets of the global custodial symmetry as follows:

$$\begin{aligned} \text{five-plet (quintet)} &\to H_5^{\pm\pm},\ H_5^{\pm},\ H_5^0; \\ \text{triplet} &\to H_3^{\pm},\ H_3^0; \\ \text{triplet} &\to H_{3M}^{\pm},\ H_{3M}^0; \\ \text{three singlets} &\to H_1^0,\ H_{1M}^0,\ H_1^{0\prime}. \end{aligned} \tag{25}$$

The above discussion about physical scalars does not depend on the specific case of Higgs potential, but works for any of those that possess $SU(2)_L \otimes SU(2)_R$ global symmetry, including the cases considered in detail in [9]. The physical Higgs bosons which are generated after the process of gauge symmetry breaking should have masses at the electroweak scale, thus in the range of 100 to a few hundred GeV. The scalars arranged in the same multiplets (not singlet) have the same masses, while three singlets H_1^0, H_{1M}^0, $H_1^{0\prime}$ are not physical states in general. These states are linear combinations of mass eigenstates, which are denoted respectively as $\tilde{H}_1^0$, $\tilde{H}_2^0$, $\tilde{H}_3^0$. Relations between physical and gauge states are expressed as $H_1^0 = \sum_i^3 \alpha_i \tilde{H}_i$, $H_{1M}^0 = \sum_i^3 \alpha_i^M \tilde{H}_i$, where $\sum_i^3 |\alpha_i|^2 = 1$ and $\sum_i^3 |\alpha_i^M|^2 = 1$. Note that the SM Higgs scalar discovered by the Large Hadron Collider (LHC) with mass 125 GeV is one of the three abovementioned mass states.

The final physical scalar to be mentioned in this study is the light singlet ϕ_s^0, which originates from the degree of freedom of the gauge singlet Higgs ϕ_S. As a singlet, ϕ_S does not break the gauge symmetry, and its VEV v_S is expected to be much lower than the electroweak scale in order to give tiny masses for the light active neutrinos. It is reasonable to take the mass of ϕ_s^0 on the same order as v_S.

2.3 The LFV vertexes

It is known that the LFV vertex does not exist in the SM at tree level, because the charged lepton mass matrix and the matrix of Yukawa couplings are diagonal at the same time, and vector gauge bosons interact only with the left-handed components of the matter fields. In this considered

scenario, vector fields interact not only with the left-handed SM fermions but also with the right-handed components of the mirror sector. Moreover, LFV interactions occur at tree level for both the charged currents and Yukawa couplings. The Lagrangian involving charged currents in this model can be written as

$$\mathcal{L}^{CC} = \mathcal{L}^{CC}_{SM} + \mathcal{L}^{CC}_{M}, \tag{26}$$

$$\mathcal{L}^{CC}_{SM} = -\left(\frac{g}{2\sqrt{2}}\right)\sum_i \bar{\psi}_i^{SM}\gamma^\mu(1-\gamma_5)[\tau^- W_\mu^+ + \tau^+ W_\mu^-]\psi_i^{SM}, \tag{27}$$

$$\mathcal{L}^{CC}_{M} = -\left(\frac{g}{2\sqrt{2}}\right)\sum_i \bar{\psi}_i^{M}\gamma^\mu(1+\gamma_5)[\tau^- W_\mu^+ + \tau^+ W_\mu^-]\psi_i^{M}, \tag{28}$$

where ψ^{SM} and ψ^{M} stand for the SM and mirror fermionic fields in the gauge basis, respectively.

The relevant Yukawa couplings between the leptons and mirror leptons with scalars which contribute to the phenomenology of the $\mu \to e\gamma$ decay in the gauge basis are listed in Table 1. To maintain good consistency with the current experimental observation and for the sake of simplicity, we suppose that the charged lepton and mirror charged lepton mixing matrices are real (thus all involved complex phases are ignored) and $U_{\ell L} = U_{\ell R} = U_\ell$, $U^M_{\ell L} = U^M_{\ell R} = U^M_\ell$. Using the relations described in Eqs. (11), (18), one easily obtains the main vertexes that contribute to our process of interest in the mass eigenstate basis. After ignoring terms which are proportional to the second order of $R_{\nu(\ell)}$, the detailed expressions are listed in Table 2 and for $(\bar{e}'_R e^{M\prime}_L \tilde{H}^0_i)$, $(\bar{e}'_L e^{M\prime}_R \tilde{H}^0_i)$, $(\bar{e}'_L e^{M\prime}_R H^0_3)$, $(\bar{e}'_R e^{M\prime}_L H^0_3)$, $(\bar{e}'_R e^{M\prime}_L H^0_{3M})$, $(\bar{e}'_L e^{M\prime}_R H^0_{3M})$ are respectively from (29) to (34):

$$-i\frac{g}{2}Y^{ML}_{\tilde{H}^0_i} = -i\frac{g}{2M_W}\left[\frac{\alpha_i}{s_2}m^d_\ell \tilde{R}_\ell + \frac{\alpha^M_i}{s_{2M}}\tilde{R}_\ell m^d_{\ell M}\right], \tag{29}$$

$$-i\frac{g}{2}Y^{MR}_{\tilde{H}^0_i} = -i\frac{g}{2M_W}\left[\frac{\alpha_i}{s_2}m^d_\ell \tilde{R}_\ell + \frac{\alpha^M_i}{s_{2M}}\tilde{R}_\ell m^d_{\ell M}\right], \tag{30}$$

$$-i\frac{g}{2}Y^{ML}_{H^0_3} = -i\frac{g}{2M_W}\left[\frac{s_M}{c_M}m^d_\ell \tilde{R}_\ell + \frac{s_M}{c_M}\tilde{R}_\ell m^d_{\ell M}\right], \tag{31}$$

$$-i\frac{g}{2}Y^{MR}_{H^0_3} = -i\frac{g}{2M_W}\left[-\frac{s_M}{c_M}m^d_\ell \tilde{R}_\ell - \frac{s_M}{c_M}\tilde{R}_\ell m^d_{\ell M}\right], \tag{32}$$

$$-i\frac{g}{2}Y^{ML}_{H^0_{3M}} = -i\frac{g}{2M_W}\left[-\frac{s_{2M}}{s_2}m^d_\ell \tilde{R}_\ell - \frac{s_2}{s_{2M}}\tilde{R}_\ell m^d_{\ell M}\right], \tag{33}$$

$$-i\frac{g}{2}Y^{MR}_{H^0_{3M}} = -i\frac{g}{2M_W}\left[\frac{s_{2M}}{s_2}m^d_\ell \tilde{R}_\ell + \frac{s_2}{s_{2M}}\tilde{R}_\ell m^d_{\ell M}\right]. \tag{34}$$

Here, the notations $U_{\rm PMNS} = U^\dagger_\ell U_\nu$, which is the famous neutrino mixing PMNS matrix, and $U^M_{\rm PMNS} = U^{M\dagger}_\ell U^M_\nu$ and $\tilde{R}_{\ell(\nu)} = U^\dagger_\ell R_{\ell(\nu)} U^M_\ell$ have been used. For simplicity, we have also neglected the complex phases in U_ℓ and U^M_ℓ.

Table 1 Vertexes that contribute to the $\ell \to \ell'\gamma$ decay rates, written in the gauge basis

Vertexes	Couplings	Vertexes	Couplings
$\bar{e}eH^0_1$	$-i\frac{m_\ell g}{2M_W s_2}$	$\bar{e}^M e^M H^0_{1M}$	$-i\frac{m^M_\ell g}{2M_W s_{2M}}$
$\bar{e}eH^0_3$	$-i\frac{m_\ell g s_M}{2M_W c_M}\gamma_5$	$\bar{e}^M e^M H^0_3$	$i\frac{m^M_\ell g s_M}{2M_W c_M}\gamma_5$
$\bar{e}eH^0_{3M}$	$i\frac{m_\ell g s_{2M}}{2M_W s_2}\gamma_5$	$\bar{e}^M e^M H^0_{3M}$	$-i\frac{m^M_\ell g s_2}{2M_W s_{2M}}\gamma_5$
$\bar{e}_R\nu_L H^-_3$	$-i\frac{m_\ell g s_M}{\sqrt{2}M_W c_M}$	$\bar{e}^M_L\nu_R H^-_3$	$-i\frac{m^M_\ell g s_M}{\sqrt{2}M_W c_M}$
$\bar{e}_R\nu_L H^-_{3M}$	$-i\frac{m_\ell g s_{2M}}{\sqrt{2}M_W s_{2M} c_M}$	$\bar{e}^M_L\nu_R H^-_{3M}$	$-i\frac{m^M_\ell g s_M}{\sqrt{2}M_W s_{2M} c_M}$

Table 2 Vertexes that contribute to the $\ell \to \ell'\gamma$ decay rates in the mass eigenstate basis

Vertexes	Couplings
$(\bar{e}'_L\gamma^\mu\chi_L)W^-_\mu$	$-i\frac{g}{\sqrt{2}}U^L_{W_\mu} = -i\frac{g}{\sqrt{2}}U_{\rm PMNS}$
$(\bar{e}'_L\gamma^\mu\chi^M_L)W^-_\mu$	$i\frac{g}{\sqrt{2}}U^{ML}_{W_\mu} = i\frac{g}{\sqrt{2}}\tilde{R}_\nu\left(U^M_{\rm PMNS}\right)^*$
$(\bar{e}'_R\gamma^\mu\chi^c_L)W^-_\mu$	$-i\frac{g}{\sqrt{2}}U^R_{W_\mu} = -i\frac{g}{\sqrt{2}}\tilde{R}^{\rm T}_\nu\left(U_{\rm PMNS}\right)^*$
$\bar{e}'_R\chi_L H^-_3$	$-i\frac{g}{2}Y^L_{H^-_3} = -i\frac{g s_M}{2M_W c_M}m^d_\ell U_{\rm PMNS}$
$\bar{e}'_R\chi^M_L H^-_3$	$i\frac{g}{2}Y^{ML}_{H^-_3} = i\frac{g s_M}{2M_W c_M}m^d_\ell\tilde{R}_\nu\left(U^M_{\rm PMNS}\right)^*$
$\bar{e}'_L\chi^{Mc}_L H^-_3$	$-i\frac{g}{2}Y^{MR}_{H^-_3} = -i\frac{g s_M}{2M_W c_M}\tilde{R}_\ell m^d_{\ell M}U^M_{\rm PMNS}$
$\bar{e}'_R\chi_L H^-_{3M}$	$-i\frac{g}{2}Y^L_{H^-_{3M}} = -i\frac{g s_{2M}}{2M_W s_{2c M}}m^d_\ell U_{\rm PMNS}$
$\bar{e}'_R\chi^M_L H^-_{3M}$	$i\frac{g}{2}Y^{ML}_{H^-_{3M}} = i\frac{g s_{2M}}{2M_W s_{2c M}}m^d_\ell\tilde{R}_\nu\left(U^M_{\rm PMNS}\right)^*$
$\bar{e}'_L\chi^{Mc}_L H^-_{3M}$	$-i\frac{g}{2}Y^{MR}_{H^-_{3M}} = -i\frac{g s_M}{2M_W s_{2M} c_M}\tilde{R}_\ell m^d_{\ell M}U^M_{\rm PMNS}$
$\bar{e}'_R e^{M\prime}_L\phi^0_s$	$-i\frac{g}{2}Y^{ML}_{\phi^0_s} = -ig_{\ell s}U^\dagger_{\ell R}U^M_{\ell L}$
$\bar{e}'_L e^{M\prime}_R\phi^0_s$	$-i\frac{g}{2}Y^{MR}_{\phi^0_s} = -i\,g_{\ell s}U^\dagger_{\ell L}U^M_{\ell R}$

3 Phenomenology of $\mu \to e + \gamma$ decay

3.1 Form factors and $\mu \to e + \gamma$ branching ratio

Before introducing the $\mu \to e + \gamma$ branching ratio, the loop integral factors must be calculated. In this work, we take into account the effective charged lepton flavor-changing operators arising at one-loop level with the participation of physical Higgs scalars (which include the single and neutral charges, heavy and light ones) and W gauge bosons. The final result can be written as

$$\mathcal{L}_{\rm eff} = -4\frac{eG_F}{\sqrt{2}}m_\mu\left(A_R\bar{e}\sigma_{\mu\nu}P_R\mu + A_L\bar{e}\sigma_{\mu\nu}P_L\mu\right)F^{\mu\nu} + \text{H.c.} \tag{35}$$

Here $A_{L,R}$ are the form factors:

$$A_R = -\sum_{H^Q,k}\frac{M_W^2}{64\pi^2 M_H^2}\left[\left(Y_H^L\right)_{\mu k}\left(Y_H^L\right)^*_{ek} G_H^Q(\lambda_k) + \frac{m_k}{m_\mu}\left(Y_H^R\right)_{\mu k}\left(Y_H^L\right)^*_{ek}\times R_H^Q(\lambda_k)\right] + \frac{1}{32\pi^2}\sum_k\left[\left(U_{W_\mu}^L\right)_{\mu k}\left(U_{W_\mu}^L\right)^*_{ek} G_\gamma(\lambda_k) - \left(U_{W_\mu}^R\right)_{\mu k}\left(U_{W_\mu}^L\right)^*_{ek}\frac{m_k}{m_\mu}R_\gamma(\lambda_k)\right], \quad (36)$$

$$A_L = -\sum_{H^Q,k}\frac{M_W^2}{64\pi^2 M_H^2}\left[\left(Y_H^R\right)_{\mu k}\left(Y_H^R\right)^*_{ek} G_H^Q(\lambda_k) + \frac{m_k}{m_\mu}\left(Y_H^L\right)_{\mu k}\left(Y_H^R\right)^*_{ek} R_H^Q(\lambda_k)\right] + \frac{1}{32\pi^2}\sum_k\left[\left(U_{W_\mu}^R\right)_{\mu k}\left(U_{W_\mu}^R\right)^*_{ek} G_\gamma(\lambda_k) - \left(U_{W_\mu}^L\right)_{\mu k}\left(U_{W_\mu}^R\right)^*_{ek}\frac{m_k}{m_\mu}R_\gamma(\lambda_k)\right], \quad (37)$$

where $H^Q = \phi_S^0, \tilde{H}_i^0$ $(i = 1,2,3)$, H_3^0, H_{3M}^0, H_3^+, H_{3M}^+, and m_k are the masses of associated fermions that along with either H^Q or W_μ form loops. The functions $G_H^Q(x)$, $R_H^Q(x)$, $G_\gamma(x)$, and $R_\gamma(x)$ appearing in Eqs. (36) and (37) are as follows

$$G_H^Q(x) = -\frac{(3Q-1)x^2+5x-3Q+2}{12(x-1)^3} + \frac{1}{2}\frac{x(Qx-Q+1)}{2(x-1)^4}\log(x), \quad (38)$$

$$R_H^Q(x) = \frac{(2Q-1)x^2-4(Q-1)x+2Q-3}{2(x-1)^3} - \frac{Qx-(Q-1)}{(x-1)^3}\log(x), \quad (39)$$

$$G_\gamma(x) = \frac{20x^2-7x+2}{4(x-1)^3} - \frac{3}{2}\frac{x^3}{(x-1)^4}\log(x), \quad (40)$$

$$R_\gamma(x) = -\frac{x^2+x-8}{2(x-1)^2} + \frac{3x(x-2)}{(x-1)^3}\log(x), \quad (41)$$

where we have defined $\lambda_k = m_k^2/M^2_{W_\mu(H^Q)}$.

Note that the monotonic functions $G_\gamma(x)$ and $R_\gamma(x)$, which are defined for the x variable varying in the interval $[0,+\infty)$, have been introduced in previous studies, for instance [17,28]. At specific points such as $x = 0$, 1 and x tend to infinity, and $G_\gamma(x)$ obtains limited values as $-1/2$, $-3/8$ and 0, respectively. Similarly, we also have $R_\gamma(x \to 0) = 4$, $R_\gamma(x \to 1) = 3/2$ and $R_\gamma(x \to \infty) = -1/2$. Compared with the form factors for the Higgs scalar one-loop that have been used in previous publications [19,28], $G_H^Q(x)$ has better expression,[1] and $R_H^Q(x)$, to the best of the author's knowledge, has not been given so far.

The branching ratio of the $\mu \to e+\gamma$ decay is easily obtained as

$$\mathrm{Br}(\mu \to e+\gamma) = 384\pi^2(4\pi\alpha_{em})\left(|A_R|^2+|A_L|^2\right), \quad (42)$$

where $\alpha_{em} = 1/137$ is the fine-structure constant.

3.2 Numerical analysis of the $\mu \to e+\gamma$ decay

In this section we numerically analyze the $\mu \to e+\gamma$ branching ratio using the current experimental data and expected sensitivity of the future experiments. Clearly, taking into account all possible contributions to the process at the same time would not be a good strategy to provide a detailed understanding of the role of each kind of diagram. Thus, we separately consider the contributions of the one-loop diagrams with virtual W gauge boson and the neutral and singly charged Higgs scalars to the ratio. For simplicity, in further numerical discussion, we suppose that three heavy neutrinos possess equal masses, denoted as m_χ^M. Similarly, three mirror charged lepton masses are m_ℓ^M.

The LFV vertexes involving neutrinos and the W boson taken up to $R_{\nu(\ell)}$ first order are the first three listed in Table 2. In fact, the contribution of light neutrinos to the $\mu \to e+\gamma$ decay is extremely small, which can be easily seen from Eq. (36). For light neutrino masses at sub-eV order or less, and $M_W = 80$ GeV, $\lambda_k = m_k^2/M_W^2 \approx 0$, which leads to (see Eq. (36))

$$\sum_{k=1}^3\left(U_{W_\mu}^L\right)_{\mu k}\left(U_{W_\mu}^L\right)^*_{ek} G_\gamma(\lambda_k) \approx \left(U_{W_\mu}^{L\dagger}U_{W_\mu}^L\right)_{e\mu} G_\gamma(0) \approx 0, \quad (43)$$

due to the unitarity of the Pontecorvo–Maki–Nakagawa–Sakata (PMNS) matrix. Moreover, the contribution from the interference term in A_R is strongly suppressed by the factor $m_k/m_\mu \sim 10^{-1}\,\mathrm{eV}/10^2\,\mathrm{MeV} \sim 10^{-9}$.

The constraint on the strength of the interaction between the heavy neutrinos and the W gauge boson by the lepton flavor violation decay $\mu \to e\gamma$ is given in Fig. 1. The blue and red lines correspond to the constraints obtained using the current upper bound or the designed sensitivity of the future experiment, respectively. The results are apparently less meaningful compared with the limits, which can be directly derived from what we already know about light neu-

[1] $G_H^Q(x)$ introduced in the current research is valid for any x in the interval $[0,+\infty)$, while the previous calculations are applied only for infinitesimal λ_k. When x tends to zero, functions $G_H^Q(x)$ tend to $1/6 - Q/4$, which is consistent with the results obtained in [19,28].

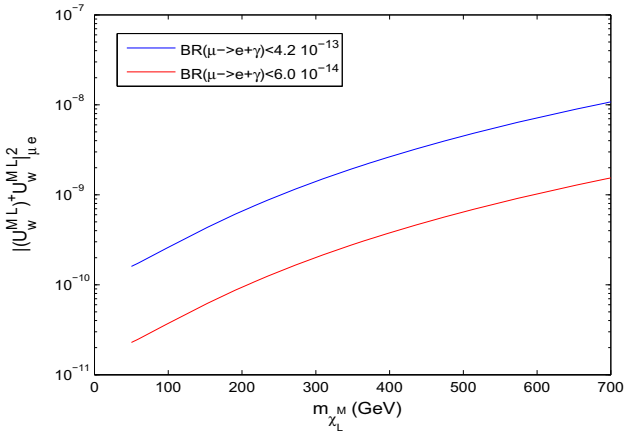

Fig. 1 Constraint on $\left(U_W^{ML\dagger}U_W^{ML}\right)_{e\mu}$ by $\mu \to e\gamma$ decay from current (blue line) and future expected (red line) sensitivities as a function of heavy neutrino mass m_χ^M

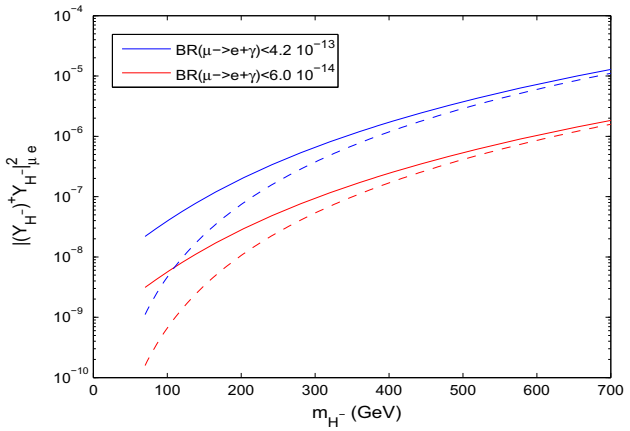

Fig. 2 Constraint on Yukawa couplings as a function of physical singly charged Higgs scalar mass by $\mu \to e\gamma$ decay if only left or right sector is taken into account, for new neutrino masses of 150 GeV (solid lines) and 10^{-9} GeV (dashed lines)

trino masses. One has

$$\tilde{m}_\nu \sim 10^{-10}\,\text{GeV} \Rightarrow R_\nu = \frac{m_\nu^D}{M_R} \sim 10^{-5}\sqrt{\frac{1\text{GeV}}{M_R}}; \qquad (44)$$

thus, $|R_\nu|^2 \sim 10^{-12}$ for $M_R \sim 100$ GeV, which is at least seven (six) orders smaller than the constraints obtained from Fig. 1: $\left|U_W^{ML\dagger}U_W^{ML}\right|_{e\mu} \sim |R_\nu|^2 < 10^{-5}$ (3×10^{-6}) corresponding to the current (near future) experimental sensitivities.

Unlike the earlier considered case, contributions of diagrams with participation of virtual Higgs scalars (both neutral and singly charged) contain fully two terms given in (36), (37). The interference term is no longer suppressed but dominates over the first term due to the large masses of accompanying particles with the physical scalar, which are heavy neutrinos or new charged leptons depending on the kind of charge

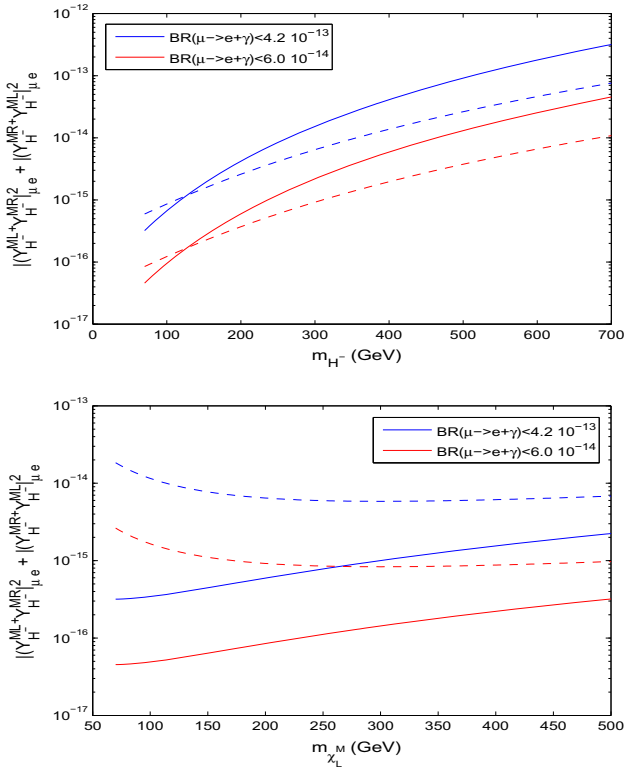

Fig. 3 Upper bounds on Yukawa couplings by $\mu \to e\gamma$ decay as functions of (i) singly charged Higgs mass (upper panel) for $m_{\chi_L^M} = 80$ (200) GeV, solid (dashed) lines; (ii) heavy neutrino masses (lower panel) for $m_{H^-} = 70$ (300) GeV, solid (dashed) lines

carried by the scalar. If heavy neutrino and new charged lepton masses, ($m_{\chi_L^M}$ and m_ℓ^M), are about hundreds GeV, then the ratio $m_k/m_\mu \sim 100$ GeV/100 MeV $\sim 10^3$, which indicates the dominated factor of the second term over the first term.

We show in Fig. 2 the constraint on the Yukawa coupling only if the first terms in (36) and (37) are taken into account for singly charged scalar cases. The stringency obtained in this case on the magnitude of the couplings is almost the same as the previous consideration of the W gauge boson and heavy neutrino couplings, and thus does not provide any new meaning. Our study shows that similar results are obtained for the case of neutral Higgs scalars.

The contributions of the first terms in the expressions of the form factors A_L and A_R are less important. This is because they are strongly suppressed by the second terms, as explained previously. Figure 3 describes the upper constraints on the relevant Yukawa couplings as a function of the Higgs scalar mass (upper panel) and heavy neutrino mass (lower panel), which are varied from about 100 GeV to several hundreds of GeV. The constraints are about six orders more stringent than the values of those obtained from the previous figure. This, once again, proves the dominant contribution of the

interference term and is also consistent with the illustration given above. The left plot shows lines which have the shape of monotonically increasing functions; therefore, the most stringent constraints on $|(Y^{ML}_{H^-})^\dagger Y^{MR}_{H^-}|^2_{\mu e} + |(Y^{MR}_{H^-})^\dagger Y^{ML}_{H^-}|^2_{\mu e}$ are at the initial points of the lines, with $m_{H^-} \sim 100$ GeV. The results read as follows:

$$\begin{aligned} &|(Y^{ML}_{H^-})^\dagger Y^{MR}_{H^-}|^2_{\mu e} + |(Y^{MR}_{H^-})^\dagger Y^{ML}_{H^-}|^2_{\mu e} \\ &\lesssim 3.0 \times 10^{-16} (6.0 \times 10^{-16}) \quad \text{for } m_{\chi^M_L} \\ &= 80\ (200)\ \text{GeV}, \end{aligned} \tag{45}$$

using the present experimental upper bound; and

$$\begin{aligned} &|(Y^{ML}_{H^-})^\dagger Y^{MR}_{H^-}|^2_{\mu e} + |(Y^{MR}_{H^-})^\dagger Y^{ML}_{H^-}|^2_{\mu e} \\ &\lesssim 4.0 \times 10^{-17} (8.0 \times 10^{-17}) \quad \text{for } m_{\chi^M_L} \\ &= 80\ (200)\ \text{GeV}, \end{aligned} \tag{46}$$

using the expected upper bound in the future.

Note that Fig. 3 is common for both H^-_3 and H^-_{3M}; however, the specific forms of Yukawa couplings involving them (see Table 2) will determine how sensitive they are with the $\mu \to e\gamma$ decay experiments. The couplings involved depend on a larger number of new parameters, where most of them are unknown, and thus it is difficult, if not impossible, to carry out a detailed analysis. In this study, we try to roughly estimate the sensitivities of the $\mu \to e\gamma$ decay with the present and future experiments, using the known data and supposing that the model is functioning at the electroweak scale.

Let us make a numerical estimation. As was explained in the earlier part, $R_\nu \sim 10^{-5}\sqrt{\frac{1\text{GeV}}{M_R}} \sim 10^{-6}$. In the same way, we also have $R_\ell \sim 10^{-5} \times \sqrt{\frac{1\text{GeV M}_\text{R}}{M^2_{\ell M}}} \sim 10^{-6}$. It is reasonable to estimate $\tilde{R}_{\ell(\nu)} = U^\dagger_\ell R_{\ell(\nu)} U^M_\ell \sim 10^{-6}$, at the same order as R_ℓ and R_ν, since the basis transformation matrices U_ℓ and U^M_ℓ are normalized. Furthermore, we take the heavy neutrino and mirror charged lepton masses at about 100 GeV. The Yukawa coupling-dependent factor of the branching ratio in Eq. (42) reads:

$$\begin{aligned} &\left|Y^{L\dagger}_{H^-_{3M}} Y^R_{H^-_{3M}}\right|^2_{21} + \left|Y^{R\dagger}_{H^-_{3M}} Y^L_{H^-_{3M}}\right|^2_{21} \\ &= \left(\frac{s_M}{s_2 c^2_M}\right)^2 \frac{\left|m^d_\ell \tilde{R}_\nu m^d_{\ell M} \tilde{R}_\ell\right|^2_{21} + \left|\tilde{R}_\ell m^d_{\ell M} \tilde{R}_\nu m^d_\ell\right|^2_{21}}{M^4_W} \\ &\sim 10^{-24} \left(\frac{s_M}{s_2 c^2_M}\right)^2 \\ &\quad \times \left(\frac{3 m_\mu m^M_\ell}{M^2_W}\right)^2 \sim 2.2 \times 10^{-29} \left(\frac{s_M}{s_2 c^2_M}\right)^2. \end{aligned} \tag{47}$$

Here we have ignored the second term (proportional to m_e), which is strongly suppressed by the first term (proportional to m_μ). This result means that the $\mu \to e\gamma$ branching ratio may be within the sensitive limit of future experiments only if s_2 and c_M are both equal to or smaller than 0.01. For the H^-_3 case, the factor $\left(\frac{s_M}{s_2 c^2_M}\right)^2$ in Eq. (47) is replaced by $\left(\frac{s^2_M}{c^2_M}\right)^2$, and thus the quantity $\left|Y^{L\dagger}_{H^-_3} Y^R_{H^-_3}\right|^2_{21}$ would reach the order of 10^{-17} if $c_M \lesssim 0.001$. These cases, however, are not realistic, for instance, if $s_2 < 0.01$, which leads to a magnitude of $v_2 \sim$ few GeV, that requires very large Yukawa couplings to give the right masses for heavy quarks, especially for the top. This is apparently disfavored by the LHC. Thus, the result is equivalent to the conclusion that the contributions of these channels to the decay rate are beyond the detectable possibilities of the current and near-future experiments.

Due to the enormous disparity between their masses, we analyze the physical phenomenology for the light and heavy neutral Higgs scalars separately. Note that the first terms of the Yukawa couplings, listed from Eq. (29) to Eq. (34), are proportional to normal charged lepton masses, and thus are ignorable in comparison with the others, which are proportional to heavier masses of the mirror leptons. We show in Fig. 4 the constraints on the relevant Yukawa couplings

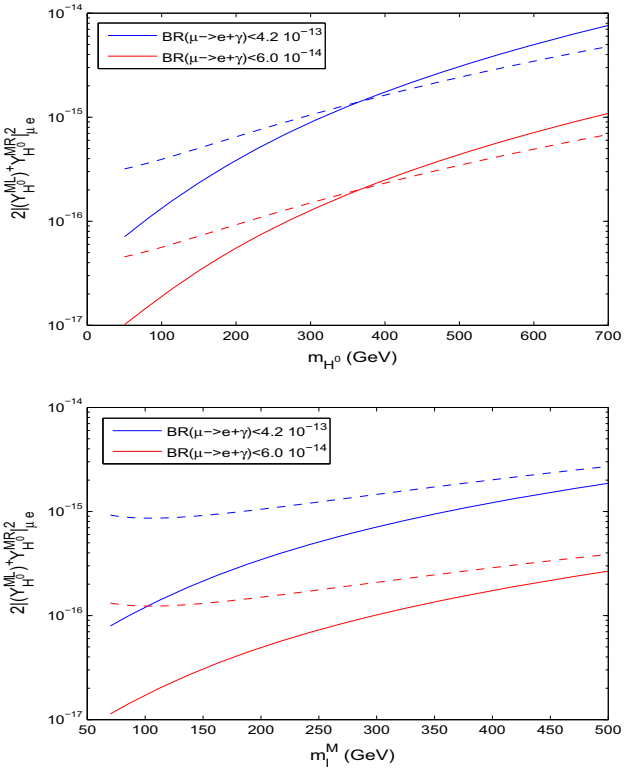

Fig. 4 Upper bounds on Yukawa couplings involving H^0 (H^0_3, H^0_{3M}, $\tilde{H}^0_i$, $(i = 1, 2, 3)$), by the $\mu \to e\gamma$ decay as a function of (i) neutral Higgs scalar mass (upper panel) for $m^M_\ell = 80\ (200)$ GeV, solid (dashed) lines; (ii) mirror charged lepton masses (lower panel) for $m_{H^0} = 70\ (300)$ GeV, solid (dashed) lines

as a function of the Higgs scalar mass (upper panel) and heavy charged lepton mass (lower panel), respectively. One can easily realize that the heavier the Higgs boson and mirror charged lepton masses, the less stringent the constraints given by $\mu \to e\gamma$ decay. Moreover, compared with the singly charged Higgs scalar cases, the constraints obtained in this case are slightly more stringent. One easily obtains from the left panel of Fig. 4 that

$$2|(Y^{ML}_{H^0})^\dagger Y^{MR}_{H^0}|^2_{\mu e} \lesssim 7.0 \times 10^{-17}(3.0 \times 10^{-16}), \quad (48)$$

for $m^M_\ell = 80\ (200)$ GeV with the present experimental upper bound, and

$$2|(Y^{ML}_{H^0})^\dagger Y^{MR}_{H^0}|^2_{\mu e} \lesssim 1.0 \times 10^{-17}(4.5 \times 10^{-17}), \quad (49)$$

for $m^M_\ell = 80\ (200)$ GeV with the future expected upper bound.

If we carry on a similar estimation as in the previous part, the results are:

$$2\left|Y^{L\dagger}_{H^0} Y^R_{H^0}\right|^2_{21} = 2\alpha^4 \times \frac{\left|\tilde{R}_\ell (m^d_{\ell M})^2 \tilde{R}_\ell\right|^2_{21}}{M^4_W} \sim 4.4 \times 10^{-23}\alpha^4, \quad (50)$$

where α stands for $\frac{\alpha_i}{s_2}$, $\frac{s_M}{c_M}$ or $\frac{s_2}{s_{2M}}$, corresponding to $\tilde{H}^0_i$, $(i = 1, 2, 3)$, H^0_3 or H^0_{3M}, respectively. Compared with Eq. (47), this result is about six orders higher (more sensitive) because the light charged lepton diagonal matrix m^d_ℓ in the earlier formula has been replaced by the heavy matrix $m^d_{\ell M}$. In the case of H^0_3, for $c_M = 0.01$, the factor $2\left|Y^{L\dagger}_{H^0} Y^R_{H^0}\right|^2_{21} \sim 4.4 \times 10^{-15}$, which is about two orders higher than the upper constraint of that if the decay signal would not be probed by the future experiment. In fact, our calculation shows that the factor might be larger than 10^{-17} with $c_M \lesssim 0.03$. We have the same conclusions if $s_2 \sim 0.01$, α_i is not small (for $\tilde{H}^0_i$) and $s_{2M} \sim 0.01$, s_2 is not small (for H^0_{3M}). Note that the contributions to the decay rate by the $\tilde{H}^0_i$ and H^0_{3M} channels are not likely to be sensitive at the same time, as they are dependent on s_2 in opposite ways.

The constraints on the Yukawa couplings involving the light Higgs scalar are shown in Fig. 5, in which the scalar mass is varied over a large range from KeV to more than 10 GeV (upper panel). The figure shows that the constrained stringency on the Yukawa couplings does not change with the increase in $m_{\phi^0_s}$ until about 10 GeV, then slowly decreases. The precise values of the upper limits obtained from the red and blue lines, respectively, are

$$2|(Y^L_{\phi^0_s})^\dagger Y^R_{\phi^0_s}|^2_{\mu e} \lesssim 4.7 \times 10^{-17}(3.0 \times 10^{-16}), \quad (51)$$

for $m^M_\ell = 80\ (200)$ GeV, and

$$2|(Y^L_{\phi^0_s})^\dagger Y^R_{\phi^0_s}|^2_{\mu e} \lesssim 6.5 \times 10^{-18}(4.2 \times 10^{-17}), \quad (52)$$

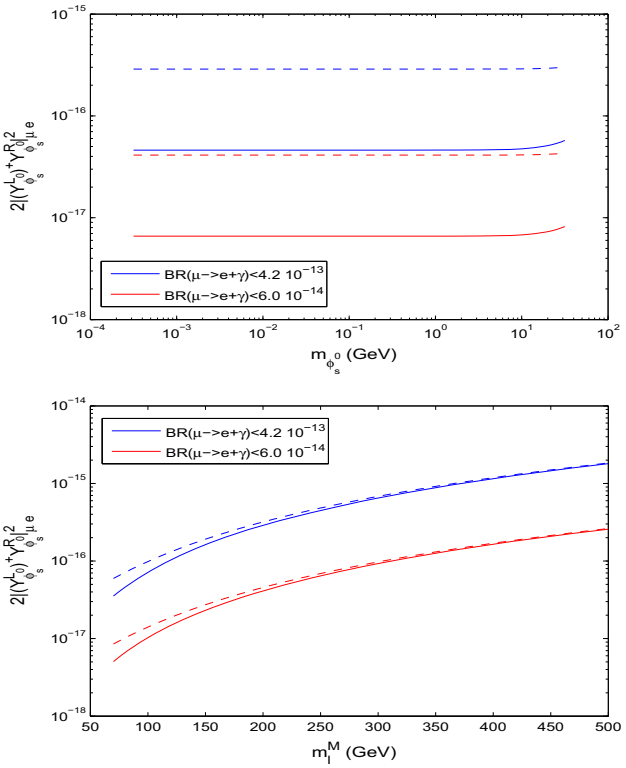

Fig. 5 The dependence of $2|(Y^L_{\phi^0_s})^\dagger Y^R_{\phi^0_s}|^2_{\mu e}$ upper limits by the current (future expected) sensitivities, corresponding to blue (red) lines, on (i) light neutral Higgs scalar mass (upper panel) for $m^M_\ell = 80\ (200)$ GeV, solid (dashed) lines; (ii) mirror charged lepton masses (lower panel) for $m_{\phi^0_s} = 10^{-3}\ (50)$ GeV, solid (dashed) lines

for $m^M_\ell = 80\ (200)$ GeV.

It can be recast from Eqs. (51) and (52), respectively, into the upper bound on $|g_{\ell s}|$ as

$$|g_{\ell s}| \lesssim 2.3 \times 10^{-5}(3.6 \times 10^{-5}) \quad \text{for } m^M_\ell = 80\ (200) \text{ GeV}, \quad (53)$$

$$|g_{\ell s}| \lesssim 1.4 \times 10^{-5}(2.3 \times 10^{-5}) \quad \text{for } m^M_\ell = 80\ (200) \text{ GeV}. \quad (54)$$

Thus, the $|g_{\ell s}|$ upper limit is estimated with current experimental data to be at the order 10^{-5}, and it might be improved slightly if the next generation of the $\mu \to e\gamma$ experiment would not probe any signal. However, the constraint is still in the same scale.

As one can see in the lower panel of Fig. 5, the constraints on the Yukawa couplings become increasingly less stringent as the mirror charged lepton mass increases. However, the shape does not strongly affect the $|g_{\ell s}|$ upper bound. Let us make a simple evaluation. For $m^M_\ell = 500$ GeV, which corresponds to the highest or the end point of each line, one has $2|(Y^L_{\phi^0_s})^\dagger Y^R_{\phi^0_s}|^2_{\mu e} \lesssim 1.8 \times 10^{-15}(2.6 \times 10^{-16})$, with ignorable dependence on the light Higgs scalar mass. The result leads to $|g_{\ell s}| \lesssim 5.7 \times 10^{-5}(3.5 \times 10^{-5})$, which is fairly close

to what was obtained in (53) and (54). This means that the energy scale of v_S (thus, also the light Higgs mass $m_{\phi_s^0}$) is on the order of GeV or more, if one wants to keep the neutrino mass generation scale at EW and ensure light active neutrino mass ($\tilde{m}_\nu \approx (m_\nu^D)^2/M_R = (g_{\ell s} v_S)^2/M_R$) of sub-eV as results have been observed experimentally.

4 Conclusion

In this work, we have performed a numerical analysis for the $\mu \to e\gamma$ decay in a scenario of the EW-scale non-sterile right-handed neutrino model, which is accommodated by the 125 GeV SM-like scalar discovery. The decay is suggested to occur at one-loop diagrams, formed by neutrinos (heavy and light) along with W boson or singly charged scalars and light or heavy neutral scalars with charged leptons. We have shown that the contribution provided by the neutrino and W boson loop channels gives a trivial upper constraint, which is about six orders less stringent than the limit of that derived directly from the currently known neutrino mass data. For the case that particles running inside loops are light scalar and mirror charged leptons, upper bound roughly derived for the magnitude of Yukawa couplings $|g_{\ell s}|$ by comparing theoretical prediction and experimental results is some number of order 10^{-5}. This brings the singlet vacuum expectation value up to a magnitude of a few GeV or few tens of GeV, if the RH neutrino mass is managed within the electroweak scale. We have also demonstrated that the branching ratio of the $\mu \to e\gamma$ decay might be large enough to reach the expected sensitivity, $\text{Br}(\mu \to e\gamma) \leq 6.0 \times 10^{-14}$, of the upgraded MEG experiment, if one of the two particles running in the loop is the heavy scalar with neutral or single charge. For instance, as one of the most promising possibilities, the magnitude of the branching ratios may be within the detectable range with $c_M \leq 0.03$ for the case of neutral scalar H_3^0 participating in the process.

Acknowledgements This research is funded by the Vietnam National Foundation for Science and Technology Development (NAFOSTED) under Grant number 103.01-2019.307.

Data Availability Statement This manuscript has no associated data or the data will not be deposited. [Authors' comment: The details could be found in the part of discussion involving the contributions of diagrams with heavy neutral scalars.]

Funded by SCOAP[3].

References

1. P.Q. Hung, A model of electroweak-scale right-handed neutrino mass. Phys. Lett. B **649**, 275–279 (2007)
2. P. Minkowski, $\mu \to e\gamma$ at a rate of one out of 10^9 muon decays? Phys. Lett. B **67**, 421–428 (1977)
3. M. Gell-Mann, P. Ramond, R. Slansky, Complex spinors and unified theories. Conf. Proc. C **790927**, 315–321 (1979)
4. T. Yanagida, Horizontal gauge symmetry and masses of neutrinos. Conf. Proc. C **7902131**, 95–99 (1979)
5. R.N. Mohapatra, G. Senjanovic, Neutrino mass and spontaneous parity nonconservation. Phys. Rev. Lett. **44**, 912 (1980)
6. V. Hoang, P.Q. Hung, A.S. Kamat, Electroweak precision constraints on the electroweak-scale right-handed neutrino model. Nucl. Phys. B **877**, 190–232 (2013)
7. G. Aad et al., Observation of a new particle in the search for the Standard Model Higgs boson with the ATLAS detector at the LHC. Phys. Lett. B **716**, 1–29 (2012)
8. S. Chatrchyan et al., Observation of a new boson at a mass of 125 GeV with the CMS experiment at the LHC. Phys. Lett. B **716**, 30–61 (2012)
9. V. Hoang, P.Q. Hung, A.S. Kamat, Non-sterile electroweak-scale right-handed neutrinos and the dual nature of the 125-GeV scalar. Nucl. Phys. B **896**, 611–656 (2015)
10. S.T. Petcov, The processes $\mu \to e + \gamma$, $\mu \to e + \overline{e}$, $\nu' \to \nu + \gamma$ in the Weinberg–Salam model with neutrino mixing. Sov. J. Nucl. Phys. **25**, 340 (1977). [Erratum: Sov. J. Nucl. Phys. **25**, 698 (1977), Erratum: Yad. Fiz. **25**, 1336 (1977)]
11. S.M. Bilenky, S.T. Petcov, B. Pontecorvo, Lepton mixing, mu → e + gamma decay and neutrino oscillations. Phys. Lett. B **67**, 309 (1977)
12. T.P. Cheng, L.-F. Li, $\mu \to e\gamma$ in theories With Dirac and Majorana neutrino mass terms. Phys. Rev. Lett. **45**, 1908 (1980)
13. A.M. Baldini et al., Search for the lepton flavour violating decay $\mu^+ \to e^+\gamma$ with the full dataset of the MEG experiment. Eur. Phys. J. C **76**(8), 434 (2016)
14. A.M. Baldini et al., The search for $\mu^+ \to e^+\gamma$ with 10^{-14} sensitivity: the upgrade of the MEG experiment (2021)
15. F. Renga, Latest results of MEG and status of MEG-II, in *20th International Conference on Particles and Nuclei* (2014)
16. J. Hisano, T. Moroi, K. Tobe, M. Yamaguchi, Lepton flavor violation via right-handed neutrino Yukawa couplings in supersymmetric standard model. Phys. Rev. D **53**, 2442–2459 (1996)
17. R. Alonso, M. Dhen, M.B. Gavela, T. Hambye, Muon conversion to electron in nuclei in type-I seesaw models. JHEP **01**, 118 (2013)
18. M. Kakizaki, Y. Ogura, F. Shima, Lepton flavor violation in the triplet Higgs model. Phys. Lett. B **566**, 210–216 (2003)
19. A.G. Akeroyd, M. Aoki, H. Sugiyama, Lepton flavour violating decays tau → anti-l ll and mu → e gamma in the Higgs triplet model. Phys. Rev. D **79**, 113010 (2009)
20. G.K. Leontaris, K. Tamvakis, J.D. Vergados, Lepton and family number violation from exotic scalars. Phys. Lett. B **162**, 153–159 (1985)
21. M. Raidal, A. Santamaria, Muon electron conversion in nuclei versus mu → e gamma: an effective field theory point of view. Phys. Lett. B **421**, 250–258 (1998)

22. E. Ma, M. Raidal, U. Sarkar, Phenomenology of the neutrino mass giving Higgs triplet and the low-energy seesaw violation of lepton number. Nucl. Phys. B **615**, 313–330 (2001)
23. S.T. Petcov, Remarks on the Zee model of neutrino mixing (mu → e gamma, heavy neutrino → light neutrino gamma, etc.). Phys. Lett. B **115**, 401–406 (1982)
24. A. Abada, C. Biggio, F. Bonnet, M.B. Gavela, T. Hambye, Low energy effects of neutrino masses. JHEP **12**, 061 (2007)
25. P.Q. Hung, Electroweak-scale mirror fermions, mu → e gamma and tau → mu gamma. Phys. Lett. B **659**, 585–592 (2008)
26. P.Q. Hung, T. Le, V.Q. Tran, T.-C. Yuan, Lepton flavor violating radiative decays in EW-scale ν_R model: an update. JHEP **12**, 169 (2015)
27. C.-F. Chang, P.Q. Hung, C.S. Nugroho, V.Q. Tran, T.-C. Yuan, Electron electric dipole moment in mirror fermion model with electroweak scale non-sterile right-handed neutrinos. Nucl. Phys. B **928**, 21–37 (2018)
28. D.N. Dinh, A. Ibarra, E. Molinaro, S.T. Petcov, The $\mu - e$ conversion in nuclei, $\mu \to e\gamma$, $\mu \to 3e$ decays and TeV scale see-saw scenarios of neutrino mass generation. JHEP **08**, 125 (2012). [Erratum: JHEP **09**, 023 (2013)]
29. D.N. Dinh, D.T. Huong, N.T. Duy, N.T. Nhuan, L.D. Thien, P. Van Dong, Flavor changing in the flipped trinification. Phys. Rev. D **99**(5), 055005 (2019)
30. D.T. Huong, D.N. Dinh, L.D. Thien, P. Van Dong, Dark matter and flavor changing in the flipped 3-3-1 model. JHEP **08**, 051 (2019)
31. M.S. Chanowitz, M. Golden, Higgs boson triplets with M (W) = M (Z) $\cos\theta\omega$. Phys. Lett. B **165**, 105–108 (1985)